Marchenko equations for acoustic Green's function retrieval and imaging in dissipative media

Evert Slob, Jan Thorbecke, and Kees Wapenaar, Delft University of Technology

SUMMARY

We present a scheme for Marchenko imaging in a dissipative heterogeneous medium. The scheme requires measured reflection and transmission data at two sides of the dissipative medium. The effectual medium is the same as the dissipative medium, but with negative dissipation. We show how the measured double-sided data can be combined to obtain the single-sided reflection response of the effectual medium. Two sets of single-sided Marchenko equations follow that are used to compute to the focusing wavefield and the Green functions. Each uses single-sided reflection responses of the dissipative and effectual medium. To start the solution for these equations an initial estimate of the dissipation is required in addition to the estimate of the travel time of the first arrival. Avoiding the estimate of dissipation of the first arrival in a low-loss medium does not have a detrimental effects on the image quality. The numerical example shows the effectiveness of this strategy.

INTRODUCTION

The wavefield at any one-way travel time inside a 1D lossless layered medium generated by a source above that medium can be obtained from the reflection response of the medium measured at a receiver above the medium. The relation between this wavefield and the single-sided reflection response is known as the Marchenko equation (Lamb, 1980). The wavefield can be obtained without any knowledge of the medium. This is an exact integral equation that has been developed for inverse scattering problems (Agranovich & Marchenko, 1963). The early applications for seismic and electromagnetic waves used scaling and stretching of the spatial coordinate to derive the corresponding integral equations (Ware & Aki, 1969; Coen, 1981). It was found that in theory the impedance could be obtained as a function of one-way travel time if the source has infinite bandwidth. Real sources have finite bandwidth and the interest dwindled. In the early 2000's Rose linked the Marchenko equation to autofocusing (Rose, 2002), thereby opening the way to think about focusing instead of inverse scattering in relation to the Marchenko equation. Focusing can be done with finite bandwidth and has potential applicability in real data problems. It was understood that the wavefield occurring in the Marchenko equation is the focusing wavefield.

Broggini & Snieder (2012) showed that autofocusing can be used to obtain the homogeneous Green function for a receiver inside the 1D medium and the source above the medium. Creating 1D homogeneous Green's functions for a virtual source or receiver at some location inside an unknown heterogeneous medium from single-sided reflection data is known for some years now (Broggini *et al.*, 2012). These studies suggested that the homogeneous Green function was necessary to focus the wavefield inside an unknown medium. For the derivation of the 3D Marchenko equation it was found that the Marchenko equation can be cast as a Green function representation for the causal Green function (Wapenaar *et al.*, 2013). Hence, having the homogeneous Green function is not a necessary condition to focus a wavefield inside an unknown medium. It was also found that the location can be specified in space avoiding the need to use scaling and stretching of coordinates. The consequence of the 3D formulation is that the scheme requires initial information to obtain a solution. The information amounts to those parts of the focusing wavefield that have a space-time overlap with the Green function. In many situations this requires an estimate of the direct wavefield from the sources above the medium to the focusing point inside the medium.

Initial applications for imaging use two uncoupled Marchenko equations. Each can be used to obtain a homogeneous Green function from which the causal Green function can be split off. These two causal Green functions can be combined to obtain the up- and downgoing parts of the Green function at the virtual receiver (Broggini *et al.*, 2014; Behura *et al.*, 2014). The upgoing and downgoing parts of the Green function can be obtained directly from a single set of coupled Marchenko equations, which halves the computational cost and from which a subsurface image can be constructed (Slob *et al.*, 2014; Wapenaar *et al.*, 2014b). The initial estimate can be more complicated than just estimating the first arrival and the effects of inaccuracies in the initial estimate as discussed in Wapenaar *et al.* (2014a) and van der Neut *et al.* (2015b). Recent advances include using Marchenko Green's function retrieval with convolutional interferometry to obtain only primary reflections from single-sided reflection data (Meles *et al.*, 2016). Extensions to elastic wavefields are being explored (Wapenaar & Slob, 2014; da Costa Filho *et al.*, 2014; Wapenaar, 2014). Then the effects of having P- and S-waves need to be considered, which creates a larger space-time window where the focusing wavefields and the Green functions will overlap.

Here we take a different way forward by introducing dissipation to the medium. All known schemes rely on the fact that the medium does not dissipate wave energy. The only approximation that occurs in lossless media is that evanescent waves are not properly accounted for, which is hardly ever a serious problem. For a dissipative medium we need to modify one of the two coupled Marchenko equations to account for the effect of dissipation. We first show that the effectual medium is the time-reversed adjoint of the dissipative medium (Wapenaar *et al.*, 2001). We show that the measured double-sided reflection and transmission responses of the dissipative medium can be combined to compute the single-sided reflection response of the effectual medium. We then make a substitution in the coupled Marchenko equations for lossless media and obtain two sets of coupled Marchenko equations for dissipative media. We briefly discuss the required a priori knowledge to compute an exact solution and how to circumvent the extra condition to run the dissipative scheme. We present a numerical example to demonstrate the effectiveness of this strategy.

THE MEASUREMENT CONFIGURATION

A dissipative medium is characterised in the frequency domain by complex density $\hat{\rho}(\mathbf{x},\omega)$ and compressibility $\hat{\kappa}(\mathbf{x},\omega)$, in which $\mathbf{x}$ denotes a point in space and $\omega = 2\pi f$ is radial frequency, with f being natural frequency. We assume that at two depth levels, $\partial\mathbb{D}_0$ and $\partial\mathbb{D}_m$, reflection and transmission responses are measured as shown in Figure 1. The reflection response to a downgoing impulsive source operating at $\mathbf{x}''_H$ on $\partial\mathbb{D}_0$ is denoted $\hat{R}^{\cup}(\mathbf{x}_0,\mathbf{x}''_0,\omega)$ while the reflection response to a upgoing impulsive source operating at $\mathbf{x}'_H$ on $\partial\mathbb{D}_m$ is denoted $\hat{R}^{\cap}(\mathbf{x}_m,\mathbf{x}'_m,\omega)$ and for flux-normalised fields the transmission responses are the same and indicated by $\hat{T}$, because they obey source-receiver reciprocity.

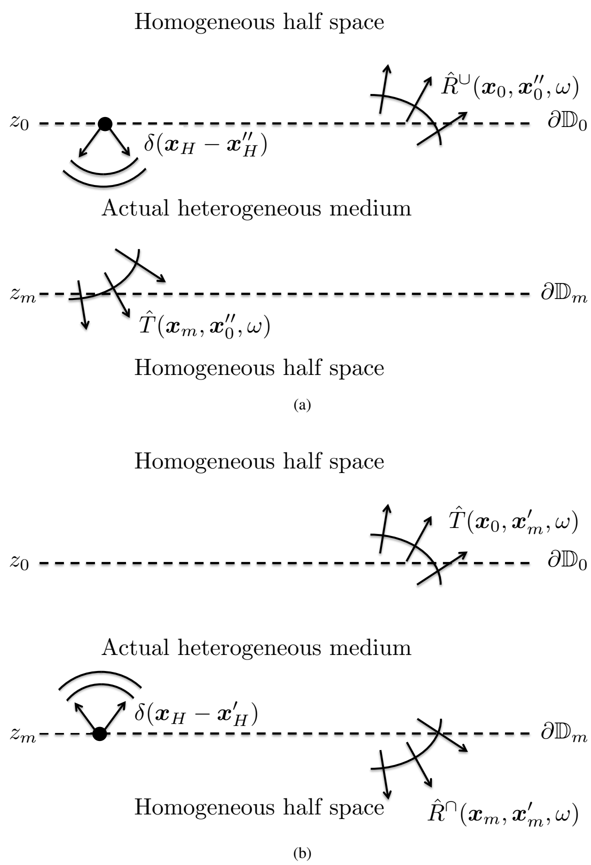

Figure 1: (a) Reflection and transmission responses from an impulsive source at $\partial\mathbb{D}_0$, (b) reflection and transmission responses from an impulsive source at $\partial\mathbb{D}_m$.

THE EFFECTUAL MEDIUM AND ITS REFLECTION RESPONSE

The effectual medium is defined as the time-reverse adjoint of the dissipative medium. It is therefore characterised by complex density $\hat{\hat{\rho}}(\mathbf{x},\omega) = \hat{\rho}^*(\mathbf{x},\omega)$ and compressibility $\hat{\hat{\kappa}}(\mathbf{x},\omega) = \hat{\kappa}^*(\mathbf{x},\omega)$, in which * denotes complex conjugation. The reflection and transmission responses in such a medium are denoted in a similar way as used for the medium parameters. They are given by $\hat{\hat{R}}^{\cup}(\mathbf{x}_0,\mathbf{x}''_0,\omega)$, $\hat{\hat{R}}^{\cap}(\mathbf{x}_m,\mathbf{x}'_m,\omega)$, and $\hat{\hat{T}}$. Because the effectual medium is the time-reverse adjoint of the dissipative medium, the complex conjugate transpose of the scattering operator matrix of the effectual medium is the inverse of the scattering operator matrix of the dissipative medium (Jaulent, 1976). Using this property of the scattering matrix we find the expression for the reflection response of the effectual medium for a source at $\mathbf{x}''_H$ at $\partial\mathbb{D}_0$ in terms of the double-sided reflection and transmission responses of the dissipative medium as

$$\int_{\partial\mathbb{D}_0} \hat{K}^*(\mathbf{x}'_m,\mathbf{x}_0,\omega)\hat{\hat{R}}^{\cup}(\mathbf{x}_0,\mathbf{x}''_0,\omega)\mathrm{d}\mathbf{x}_0 = -\left[\int_{\partial\mathbb{D}_m} \hat{R}^{\cap}(\mathbf{x}'_m,\mathbf{x}_m,\omega)[\hat{T}(\mathbf{x}_m,\mathbf{x}''_0,\omega)]^{-1}\mathrm{d}\mathbf{x}_m\right]^*, \quad (1)$$

in which

$$\hat{K}(\mathbf{x}'_m,\mathbf{x}_0,\omega) = \hat{T}(\mathbf{x}'_m,\mathbf{x}_0,\omega) - \int_{\partial\mathbb{D}_m} \hat{R}^{\cap}(\mathbf{x}'_m,\mathbf{x}_m,\omega) \int_{\partial\mathbb{D}_0} [\hat{T}(\mathbf{x}_m,\mathbf{x}'_0,\omega)]^{-1}\hat{R}^{\cup}(\mathbf{x}'_0,\mathbf{x}_0,\omega)\mathrm{d}\mathbf{x}'_0\mathrm{d}\mathbf{x}_m. \quad (2)$$

$\hat{K}(\mathbf{x}'_m,\mathbf{x}_0,\omega)$ in equation 2 and the right-hand side of equation 1 are expressed in terms of the double-sided data and can be computed after which equation 1 can be solved for the reflection response $\hat{\hat{R}}^{\cup}(\mathbf{x}_0,\mathbf{x}''_0,\omega)$. The reflection responses $\hat{R}^{\cup}$ and $\hat{\hat{R}}^{\cup}$ are needed to develop the Marchenko equations for a dissipative medium.

MARCHENKO EQUATIONS, GREEN'S FUNCTION RETRIEVAL, AND IMAGING

To derive coupled Marchenko equations in lossless media reciprocity theorems of time-convolution and time correlation types are used. The theorem of the time-convolution type can be used in dissipative media as well and leads to the well-known first equation

$$\hat{G}^-(\mathbf{x}_i,\mathbf{x}''_0,\omega) = \int_{\partial\mathbb{D}_0} \hat{R}^{\cup}(\mathbf{x}'_0,\mathbf{x}''_0,\omega)\hat{f}_1^+(\mathbf{x}'_0,\mathbf{x}_i,\omega)\mathrm{d}\mathbf{x}'_0 - \hat{f}_1^-(\mathbf{x}''_0,\mathbf{x}_i,\omega), \quad (3)$$

where $\hat{G}^-(\mathbf{x}_i,\mathbf{x}''_0,\omega)$ denotes the upgoing part of the Green function at $\mathbf{x}_i$ for a source at $\mathbf{x}''_0$ in the dissipative medium. The reciprocity theorem of the time-correlation type must be used for the focusing wavefield in the dissipative medium together with the measurement state in the effectual medium, because these media are each other's time-reversed adjoints. This means that the reflection response and Green function for the downgoing field at the virtual receiver in $\mathbf{x}_i$ that occur in the lossless scheme are replaced by their effectual medium counterparts. The second equation for the focusing wavefield in the dissipative medium is therefore given by

$$\hat{\hat{G}}^+(\mathbf{x}_i,\mathbf{x}''_0,\omega) = -\int_{\partial\mathbb{D}_0} \hat{\hat{R}}^{\cup}(\mathbf{x}'_0,\mathbf{x}''_0,\omega)[\hat{f}_1^-(\mathbf{x}'_0,\mathbf{x}_i,\omega)]^*\mathrm{d}\mathbf{x}'_0 + [\hat{f}_1^+(\mathbf{x}''_0,\mathbf{x}_i,\omega)]^*, \quad (4)$$

where $\hat{\hat{G}}^+(\mathbf{x}_i,\mathbf{x}''_0,\omega)$ denotes the downgoing part of the Green function at $\mathbf{x}_i$ for a source at $\mathbf{x}''_0$ in the effectual medium. Similar equations can be obtained for the focusing wavefield $\hat{\hat{f}}_1^{\pm}$

in the effectual medium by replacing all quantities in the dissipative medium with the corresponding ones in the effectual medium and vice versa. These equations are not given here for brevity.

In the time domain we can see that the Green functions in the dissipative and effectual medium are causal and zero valued before the direct arrival. For those time values we have the Marchenko equations for the focusing wavefield in the dissipative medium given by

$$f_1^-(\mathbf{x}_0'', \mathbf{x}_i, t) = \int_{\partial\mathbb{D}_0} \int_{-\infty}^{t} R^{\cup}(\mathbf{x}_0', \mathbf{x}_0'', t - t') f_1^+(\mathbf{x}_0', \mathbf{x}_i, t') \mathrm{d}t' \mathrm{d}\mathbf{x}_0', \tag{5}$$

$$f_1^+(\mathbf{x}_0'', \mathbf{x}_i, -t) = \int_{\partial\mathbb{D}_0} \int_{-\infty}^{t} \bar{R}^{\cup}(\mathbf{x}_0', \mathbf{x}_0'', t - t') f_1^-(\mathbf{x}_0', \mathbf{x}_i, -t') \mathrm{d}t' \mathrm{d}\mathbf{x}_0', \tag{6}$$

valid for $t < t_d(\mathbf{x}_i, \mathbf{x}_0'')$, in which $t_d(\mathbf{x}_i, \mathbf{x}_0'')$ is the time instant of the first arrival. Equations 5 and 6 are the coupled Marchenko equations for the focusing wavefield in the dissipative medium. These equations can be solved in the same way as is customary for the lossless scheme, which involves an estimate of the first arrivals at time instants $t_d(\mathbf{x}_i, \mathbf{x}_0')$. The downgoing part of the focusing function at $t = t_d(\mathbf{x}_i, \mathbf{x}_0')$ occurs in the right-hand side of equation 5 but is unknown and cannot be retrieved from these equations. The first difference compared to the lossless scheme is that the reflection response of the effectual medium occurs in equation 6 to account for dissipation in the reflection response occurring in equation 5. The second difference with the lossless scheme is that the estimate of the amplitude of the direct arrival is more complicated than in the lossless scheme. Included in the estimate of the downgoing part of the focusing wavefield at that time instant is an estimate of the dissipation along the path from $\mathbf{x}_0'$ to $\mathbf{x}_i$. Such an estimate is difficult to obtain from the data and we proceed without making such estimate. The consequence is that offset dependent amplitude errors will be introduced, which may lead to artefacts due to incomplete focusing and errors in the multiple elimination process. Remnants of multiples will then be imaged and adaptive subtraction strategies may reduce this problem (van der Neut *et al.*, 2015a).

Equations 5 and 6 are solved for the focusing wavefield in the dissipative medium and a similar set of coupled equations is solved for the focusing wavefield in the effectual medium. Once these are obtained the upgoing part of the Green function in the dissipative medium and the downgoing part of the Green function in the effectual medium can be computed using equations 3 and 4. A similar set can be used for the other two parts of the Green functions. For both media the standard imaging approaches of multidimensional deconvolution can be used (Wapenaar *et al.*, 2014b). This results in two images that have incorrect amplitudes due to the zero-dissipation estimate of the first arrival. In the dissipative medium the initial part of the downgoing focusing wavefield should compensate for the dissipation from the source to the virtual receiver. By not making an estimate for the dissipation in the initial part of the downgoing focusing wavefield its amplitude is too weak. This results in incomplete focusing and remnants of the multiples in the data will end up in the image. For a low-loss medium the effects are not too severe and a better image is produced compared to using the lossless Marchenko scheme. This is illustrated in the example below.

NUMERICAL EXAMPLE

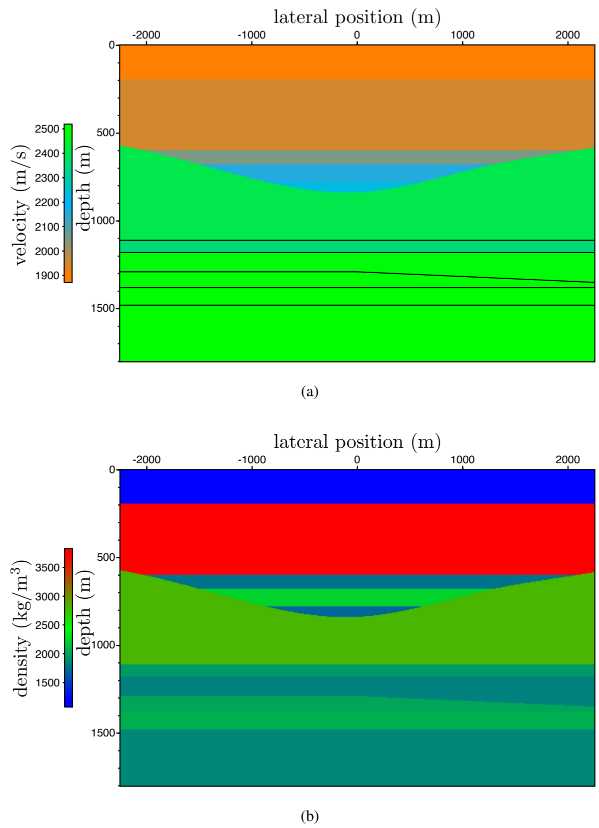

Figure 2: (a) Velocity model, (b) density model.

For the numerical example we use the model of Wapenaar *et al.* (2014b), but with dissipation added to the model. The acoustic velocities and densities in the different layers in the model are depicted in Figure 2. It consists of a layered model with increasing velocities and variable densities with a smooth syncline, below which one interface shows a dip in the right-hand side of the model. The medium parameters are chosen as a Maxwell model, $\hat{\rho} = \rho(\mathbf{x})(1 - \mathrm{j}/\omega)$ and $\hat{\kappa} = \kappa(\mathbf{x})(1 - \mathrm{j}/\omega)$. This leads to frequency independent phase velocity and a quality factor that is proportional to frequency, $Q = \omega/2$. We are interested in imaging the layered structure below the syncline and the imaged area is shown in Figure 3 with the velocities. We have computed surface reflection data for the dissipative and effectual media with a 20 Hz Ricker wavelet as the source signature. These two reflection responses are used to compute the focusing wavefields in the dissipative and effectual medium. No estimate of the attenuation has been used for the initial estimate of the focusing wavefield. Once the focusing wavefields are known, the up- and downgoing parts of the Green functions in the dissipative medium are computed. An image is computed using these Green functions in the multi-dimensional deconvolution scheme. The image is shown in Figure 4. The expected reflectors are properly imaged, but some artefacts are visible as well. Around 1630 m depth a ghost reflector is visible albeit at reduced amplitude, and very small remnants of multiples generated by the syncline structure can be seen in the image. We have also used the lossless

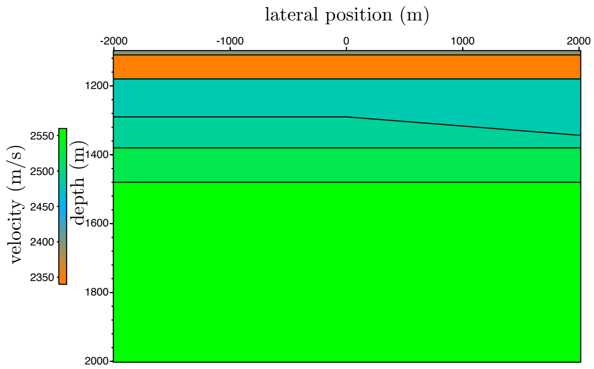

Figure 3: Part of the velocity model to be imaged.

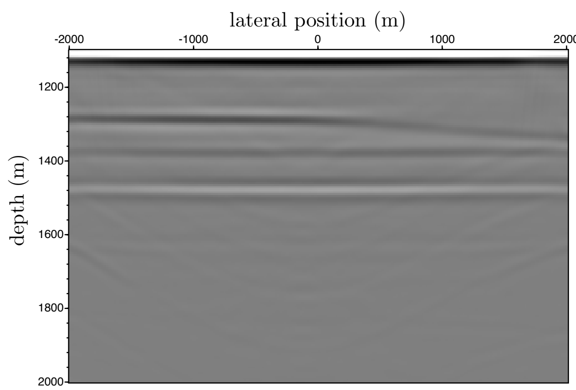

Figure 4: The image obtained with the new scheme.

Marchenko scheme on the reflection response of the dissipative medium, using the same initial estimate for the focusing wavefield, and computed the image in the same way. We have also run a conventional migration scheme on the same reflection data. Both images are shown in Figure 5. It can be seen in Figure 5a that the image has more ghosts reflectors than the image of Figure 4, especially in the region of interest between 1200 m and 1500 m depth and the artefacts seen in Figure 4 are stronger in Figure 5a. As expected the standard image of Figure 5b is severely contaminated with ghost images coming from multiples in the overburden and the target zone.

The new scheme can only be implemented when double sided reflection and transmission data are available. This is feasible in a laboratory set up, but it is not feasible in the field. Figure 5a shows that using only the reflection response of the dissipative medium a reasonable image can be produced that has much less artefacts than the conventional image. Adaptive subtraction techniques might be helpful in reducing further the artefacts that are present in the image. The present example has a constant Q-value throughout the model and at the central frequency of the wavelet $Q = 63$, which is a reasonable Q-value for many materials. This suggests that the lossless scheme could be used for seismic data, because other errors in the estimate of the direct arrival of the focusing wavefield will cause similar errors in the image. When dispersion becomes strong the lossless scheme is likely to become less effective.

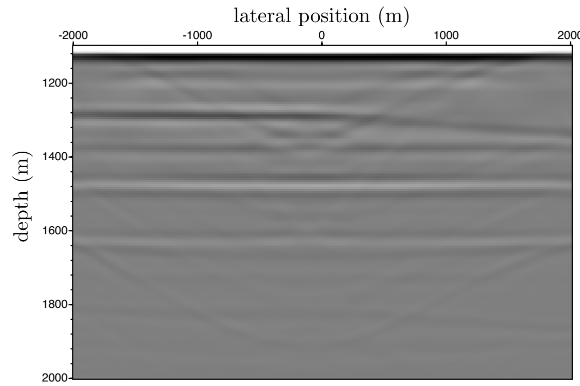

(a)

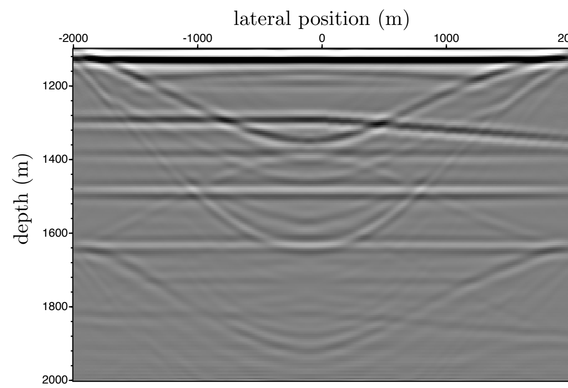

(b)

Figure 5: (a) Image using the lossless Marchenko scheme, (b) image using standard migration.

CONCLUSIONS

We have presented a Marchenko imaging scheme for a dissipative medium. This scheme is capable of creating an image that is almost free of artefacts due to multiples in the overburden. The scheme requires double-sided reflection and transmission data. These data contain redundant information and the reduction is achieved by combining all the data to compute the single-sided reflection response of the effectual medium that corresponds to the dissipative medium.

The computational cost and the amount of information needed in the scheme is therefore just twice the cost of the lossless scheme. For the model shown with a realistic quality factor the lossless Marchenko scheme produced a reasonably good quality image, which can be improved by prior Q-compenstation techniques. That is of interest because double-sided data are not going to become available from the field.